Influence of cooling rates on temperatures phase transitions and on microstructure of aluminium alloy EN AW-5083

Dolić, Natalija; Medved, J.; Mrvar, P.; Unkić, Faruk

Source / Izvornik: **Materialwissenschaft und Werkstofftechnik, 2012, 43, 957 - 964**

Journal article, Published version
Rad u časopisu, Objavljena verzija rada (izdavačev PDF)

https://doi.org/10.1002/mawe.201200929

Permanent link / Trajna poveznica: https://urn.nsk.hr/urn:nbn:hr:115:062151

Influence of cooling rates on temperatures phase transitions and on microstructure of aluminium alloy EN AW-5083

Einfluss der Abkühlgeschwindigkeit auf die Temperatur der Phasenänderung und auf die Mikrostruktur der Aluminiumlegierung EN AW-5083

N. Dolić[1], J. Medved[2], P. Mrvar[2], F. Unkić[1]

The casting of different forms and dimensions of aluminium alloy EN WA-5083 test samples and the usage of different types of mould materials resulted in achieving different cooling rates of samples. The methods used were simple thermal analysis, using casting into a measuring cell made by the Croning process and using casting into a cone-shaped measuring cell, as well as simultaneous thermal analysis using the method of differential scanning calorimetry. Significant temperature phase transitions and times of solidification were determined, and the dependence model of the solidification time on the sample cooling rate was obtained. Determining the mean number of grains per unit area on samples after having performed the simple thermal analysis and differential scanning calorimetry makes it possible to develop a dependence model of the mean number of grains per unit area on the cooling rate. These models are the basis for carrying out numerical simulations of solidification and microstructure development in the cone-shaped measuring cell, and the comparison of the distribution of the mean number of grains per unit area obtained by simulation with the one obtained experimentally. The obtained results represent a part of the preliminary tests of the microstructure development of industrially cast ingots of EN AW-5083 alloy depending on the local ingot cooling rate.

Keywords: EN AW-5083 aluminium alloy / numerical simulation / thermal analysis methods / mean number of grains per unit area

Beim Gießen verschiedener Versuchsmuster mit unterschiedlichen Formen und Größen der Aluminiumlegierung EN WA-5083 und Verwenden verschiedener Formstofftypen, wurden unterschiedliche Abkühlgeschwindigkeiten festgestellt. Dabei wurde die Methode der einfachen Thermalanalyse angewendet, die beim Gießen in eine Messzelle einmal mit dem Croning-Verfahren hergestellt wurde und einmal in eine kegelförmige Messzelle gegossen wurde, samt gleichzeitiger Thermalanalyse mit der Methode der differenzierten Wärmemessung. Dabei wurden die Temperaturphasenübergänge und Zeiten bis zur Erstarrung ermittelt sowie das Zeit-Modell in Abhängigkeit der Abkühlgeschwindigkeit bis zur Erstarrung der Versuchsprobe ermittelt. Durch die Bestimmung des Mittelwertes der Anzahl der Körner pro Fläche auf der Versuchsprobe nach der durchgeführten einfachen Thermalanalyse und der Methode der differenzierten Wärmemessung, kann ein Abhängigkeitsmodell des Mittelwertes der Anzahl der Körner pro Fläche über die Abkühlgeschwindigkeit erstellt werden. Diese Modelle sind die Basis, um die numerische Simulation des Festwerdens und die Mikrostruktur-Entwicklung in der kegelförmigen messenden Zelle, samt der Simulation des Vergleichs der Verbreitung des Mittelwertes der Anzahl von Körnern pro Fläche zu erlangen. Die erhaltenen Ergebnisse repräsentieren einen Teil der Forschung der Mikrostruktur-Entwicklung beim industriellen Gießen von Blöcken der Legierung EN AW-5083 in Abhängigkeit der lokalen Abkühlgeschwindigkeit der Blöcke.

Schlüsselwörter: EN AW-5083 Aluminiumlegierung / numerische Simulation / Thermalanalyse / Mittelwert der Anzahl von Körnern pro Fläche

[1] Faculty of metallurgy, University of Zagreb, Sisak, Croatia
[2] Faculty of Natural Science and Engineering, University of Ljubljana, Department for Materials and Metallurgy, Ljubljana, Slovenia

Corresponding author: Natalija Dolic, D.Sc., Faculty of Metallurgy, University of Zagreb, Aleja narodnih heroja 3, 44103 Sisak, Croatia
E-mail: ndolic@simet.hr

1 Introduction

The EN AW-5083 alloy, chemical symbol AlMg4.5Mn0.7 is a moderate strength aluminium alloy containing magnesium and manganese additions. [1]. The combination of alloying elements provides good corrosion resistance, even in salt water, good mechanical properties, high toughness, good weldability using various techniques [2].

The 5xxx group aluminium alloys are widely used in the manufacture of unfired, welded pressure vessels, marine, auto aircraft cryogenics, drilling rigs, TV towers, transportation equipment, and in missile components, etc.

Because of new and special applications all the production chain participants are constantly facing increasingly strict requirements regarding the material quality, i. e. its high homogeneity of the chemical composition and structure, narrow geometrical tolerances, as well as its physical, mechanical and technological properties. These are evaluated and accepted only after having met the strictest criteria of the advanced methods of testing and statistical processing of the test results.

The homogeneous structure and equiaxed grains contribute to the improvement of many properties of the cast metal, increased thermal workability and shaping during subsequent rolling or extrusion [3–5]. The grain structure (mean grain size, their distribution and morphology) has great influence on reducing the incidence of surface defects, e. g. hot and cold cracks in the ingot marginal zone [6]. The semi-continuous vertical direct water cooling process ("Direct Chill") is of great significance in the production of commercial aluminium alloys, especially in the production of large-dimension ingots, which are subsequently thermo-mechanically treated to obtain final products (rolled plates, sheets, foils, pipes, bars, billets, wires) [7–9].

The numerical simulation of Al-ingot casting and solidification by means of simulation software for the casting processes can be used to optimize the casting and solidification process. The simulation allows the analysis of casting, solidification, temperatures in the moulded item and the mould, charging and solidification times, melt rate, pressure, stress and strain in the moulded item and tools, and the porosity of the moulded items.

2 Experimental part

The objective of this paper is to use the experimentally obtained values in order to find the model of dependence of the solidification time of EN AW-5083 alloy on the cooling rate, r_c i. e. the model of dependence of the mean number of grains per unit area, $\overline{N}_A$ on the cooling rate. Within this test the cooling rates ranged from 0.17–40.3 °C/s.

Different cooling rates of samples were measured and determined by means of casting of different forms of samples and by using different types of mould materials. The methods used were simple thermal analysis (STA) and differential scanning calorimetry (DSC).

After having performed the simple thermal analysis and the differential scanning calorimetry of samples, the mean number of grains per unit area, $\overline{N}_A$ was determined. Based on the obtained results the dependence model of the mean number of grains per unit area on the obtained cooling rates was developed.

Table 1. Chemical composition of the tested EN AW-5083 alloy, charge 3116

Tabelle 1. Chemische Zusammensetzung der getesteten Legierung EN AW-5083, Charge 3116

Element compositions/wt.%									
Si	Fe	Cu	Mn	Mg	Cr	Zn	Ti	Be	Na
0.14	0.38	0.01	0.43	4.56	0.11	0.006	0.021	0.0057	0.0012

The methods of simple thermal analysis and differential scanning calorimetry were used to determine the significant phase transition temperatures (liquidus, T_L and solidus, T_S temperatures, the separation temperature of the first, T_{E1} and the second T_{E2} eutectics) and the time of solidification, Δt_s at certain cooling rates. Thus, the dependence model of the time of solidification on the cooling rate was obtained.

These obtained models allow the implementation of the simulation of casting and solidification in a cone-shaped measuring cell, and the comparison of the distribution of the number of grains obtained by simulation with the one obtained by experiment. The cone simulation is a preliminary test which will allow simulation of the development and growth of the crystal grains in the industrially cast ingot depending on the local cooling rate.

2.1 Experimental method

Tests were carried out on a sample of an ingot cast by semi-continuous vertical direct water cooling process ("Direct Chill"), of dimensions: 520 × 1680 × 4809 mm, produced from charge 3116 of EN AW-5083 alloy. The chemical composition of the tested charge was determined by the optical emission spectrometer, *Table 1*. The sample for the chemical analysis was taken during casting at ingot lengths of about 0.5 m.

The structure of the tested charge 3116 contains a significantly higher share of technological waste compared to the primary aluminium, in a ratio of 75:25%. The main components of the technological waste are alloys EN AW-1050, EN AW-5049 and EN AW-5754. In order to guarantee the expected quality of hard wrought ingots from EN AW-5083 alloy, all the components of the insert charge, including also the pure metals and master alloy for alloying, are of certified quality.

Before casting, the melt was refined by argon and chlorine mixture in an ALPUR unit. The grain refinement was performed by adding AlTi5B master alloy in the form of small bars (in the melting furnace) and wires (into the groove in front of ALPUR), in the average quantity of 1.74 kg/t of the melt [10]. The equipment for vertical semi-continuous ingot casting is based on highly automated systems. This ensures the repeatability of the target quality with high level of reliability, excluding possible operator's errors.

From the ingot cast in this way, an approximately 30 mm thick transversally cut plate was taken from its front part, after having disposed of the technological waste of approximately 200 mm at the beginning of casting. From the cut plate, from its edge, a part

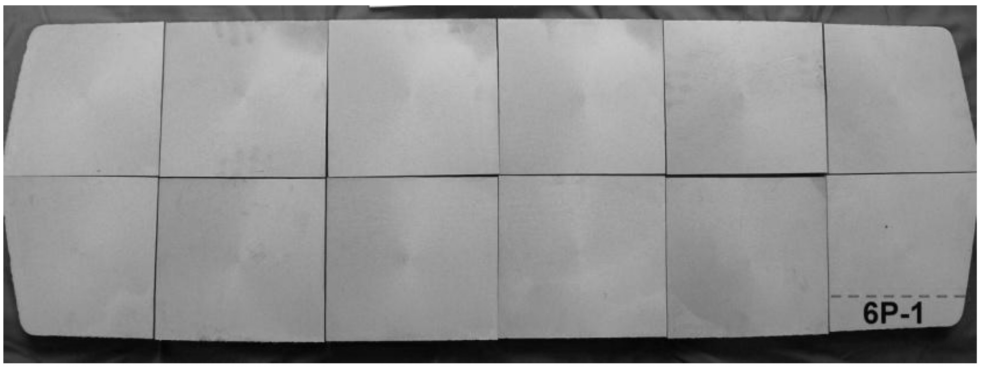

Figure 1. Schematic presentation of the location of taking the sample from the plate taken from the front part of alloy ingot EN AW-5083.

Bild 1. Schematische Darstellung der Muster-Probenentnahme, am vorderen Ende des Legierungsblocks EN AW-5083.

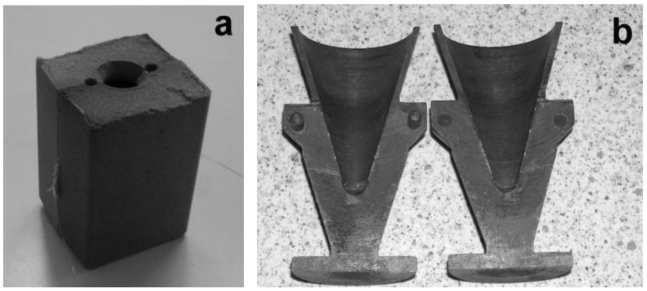

Figure 2. Measuring cells: a) Measuring cell made by Croning process, b) Cone-shaped measuring cell of gray cast iron.

Bild 2. Mess-Zellen, a) Mess-Zellen hergestellt mit dem Croning-Prozess, b) Kegelförmige Messzelle von grauem Gusseisen.

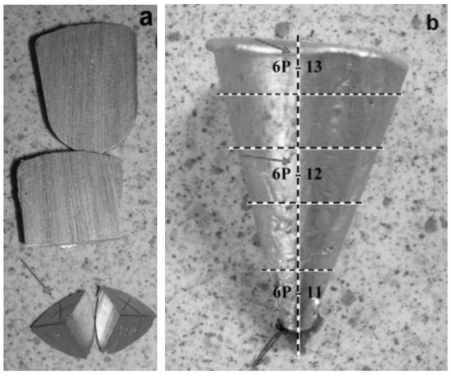

Figure 3. Methodology of sampling with spots where analysis was performed marked by arrows: a) Photo of the cut sample cast into the measuring cell made by Croning process with marked spot of taking the sample and description, b) Photo of the cut sample cast into the cone-shaped measuring cell with marked spots of taking samples and description.

Bild 3. Methode der Probenentnahme mit Kennzeichnung Analysestelle, a) Abbildung der ausgeschnittenen Versuchsprobe, gegossen in die Messzelle mit dem Croning-Prozess mit Kennzeichnung der Entnahme und Beschreibung, b) Abbildung der ausgeschnittenen Versuchsprobe, gegossen in die kegelförmige Messzelle mit Kennzeichnung der Entnahme und Beschreibung.

of the ingot was taken and used to perform tests of simple thermal analysis and differential scanning calorimetry, *Figure 1*.

In order to achieve different cooling rates and to determine the influence of the cooling rate on the significant phase transition temperatures and times of solidification, and on the mean number of grains per unit area the following analyses were performed: the simple thermal analysis using casting into the measuring cells made by the Croning process and using casting into the cone-shaped measuring cell, and the differential scanning calorimetry. Thus, different, experimentally measured cooling rates were achieved, followed by testing of these samples regarding the mean number of grains per unit area, i.e. the ASTM grain size number, *G*.

Simple thermal analysis was performed on sample 6P-1 taken from the front of the cast ingot of charge 3116, according to the scheme in Figure 1. Sample 6P-1 was molten in the graphite pot in an electric furnace. When the melt reaches the temperature of approximately 730 °C, it is poured from the graphite pot into two measuring cells: into a cell made by the Croning process (equipped with a single thermo-element in the middle), *Figure 2*a, and into a cone-shaped measuring cell, Figure 2b. Simple thermal analysis on sample 6P-1 cast into the measuring cell made by the Croning process was repeated twice (a, b), and the mean values of characteristic temperatures were taken. For the characterization of solidification of sample 6P-1 at different cooling rates a cone-shaped measuring cell of grey cast iron was used with three thermo-elements installed in it. The thermo-elements are Ni-Cr-Ni, type K. The described measuring cells are presented in Figure 2.

From the test sample cast into the measuring cell produced by the Croning process, a sample was taken for metallographic testing of determining the mean number of grains per unit area, from a precisely determined spot where the thermo-element was located (sample 6P-1, STA), *Figure 3*a. From the sample cast into the cone-shaped measuring cell three samples were taken, one from the cone base (sample 6P-13), one from the middle (sample 6P-12), and one from its vertex (sample 6P-11), which were also used to test the mean number of grains per unit area, i.e. the grain size, Figure 3b. The described sampling methods are presented in Figure 3.

The cooling curves were obtained by monitoring the cooling and solidification rates using the data acquisition instrument equipped with the measuring card DAQ Pad-MI0-16XE-50 and

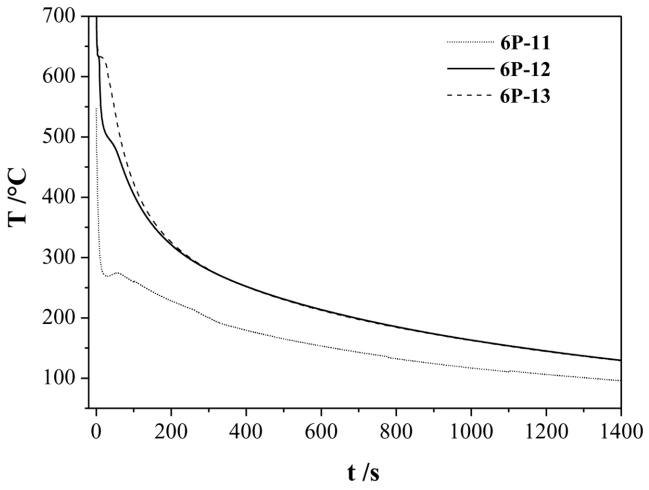

Figure 4. Cooling curves of sample 6P-1 cast in cone-shaped metal gray iron die cast.

Bild 4. Die Abkühlungskurven der Probe 6P-1, gegossen in eine kegelförmige Metallform.

the corresponding LabView 7.0 software. The cooling curves and their first and second derivation were then plotted and processed using Origin 7.0 software, which resulted in determining of the significant temperature phase changes in solidification of actual samples.

Due to different geometries, dimensions and materials of measuring cells different intensities of heat conduction are achieved resulting in different cooling rates of the test samples. The cooling rate is determined from the cooling curve from the beginning of cooling until the first change in the cooling curve gradient marking the beginning of solidification.

Simultaneous thermal analysis was carried out on sample 6P-1 using the differential scanning calorimetry method on the instrument NETZSCH STA 449C Jupiter, by means of heating and cooling technique, in order to determine adequate significant temperatures of phase transitions and solidification intervals.

Two crucibles are connected to the platinum sensor of the STA 449 instrument. The test sample is placed into one crucible as reference the Al_2O_3 crucible is used, in which, during testing, there is no reaction that would cause absorption or release of heat or change of mass. The measuring occurs in protective atmosphere of inert gas 99.999% Ar. The sample is heated to a temperature of 720 °C at a rate of 0.17 °C/s, at the same as the cooling rate to the room temperature. After that, sample is used to measure the mean number of grains per unit area (sample 6P-1, DSC).

The cooling curves obtained by simple thermal analysis and differential scanning calorimetry determine significant temperature phase transitions, i. e. times of solidification which yield the correlation between the experimentally determined times of solidification and the cooling rates.

The mean number of grains per unit area of samples after simple thermal analysis (6P-1, STA; 6P-11; 6P-12; 6P-13) and differential scanning calorimetry (6P-1, DSC) was determined by using optical microscope Olympus GX51 which was equipped with an automatic image processing system ("AnalySIS® Materials Research Lab"). In this way the dependence model of the mean number of grains per unit area on the experimentally obtained cooling rates was obtained.

Prior to the very determining of the mean number of grains the samples were subjected to the standard preparation procedure with electrolytic etching in the Barker's reagent at different etching times depending on the sample itself.

The simulation program "ProCast" was used to carry out the simulation of casting, solidification and occurrence and growth of crystal grains for the cone-shaped measuring cell.

The parameters obtained by the performed cone simulation will be used for further simulation of the distribution of the number of grains in the industrially cast EN AW-5083 alloy ingot, and for obtaining the mathematical model of dependence of the mean number of grains per unit area on the local cooling rates in the ingot.

3 Results and discussion

3.1 Results obtained by simple thermal analysis (STA)

The cooling curves of sample 6P-1 cast into metal gray iron cone-shaped die cast are presented in *Figure 4*. The cooling curve of the sample from the cone vertex is designated by 6P-11, from the middle of the cone 6P-12, whereas the one of the sample taken from the cone base is designated as 6P-13.

Cooling curves in Figure 4 indicate a significant mutual deviation in the values of significant temperatures of phase changes, as well as of the curve gradient which points to significant differences in the cooling rates. The curve of sample 6P-13 features least variation in temperature values, and with its smallest gradient it also has the lowest cooling rate of r_c = 10.8 °C/s. Using the first and the second cooling curve derivation the liquidus of temperatures T_L = 632.7 °C, separation temperatures of the first and the second eutectics T_{E1} = 607.6 °C and T_{E2} = 570.9 °C, as well as the solidus of temperatures T_S = 540.9 °C have been determined. The time of solidification for this cooling rate of sample 6P-13, as the difference of times at which the liquidus and solidus of temperatures occur, amounts to Δt_s = 65 s.

The curve of sample 6P-12 indicates the cooling rate of r_c = 40.3 °C/s, and here the following temperatures of phase transitions have been obtained: T_L = 634.0 °C, T_{E1} = 594.0 °C, T_{E2} = 544.0 °C and T_S = 523.7 °C. There is a marked fall in all temperatures compared to the previous cooling rate of 10.8 °C/s, except for T_L whose deviation is minimal and amounts to ~ 1.3 °C. In this case the solidification is completed in Δt_s = 11.2 s.

The curve of sample 6P-11 shows sample cooling at a rate of r_c= 124.0 °C/s which makes the oscillations more pronounced, and there is uncertainty in determining the appropriate respective phase transition temperatures.

After having performed casting into a cone-shaped die cast on samples 6P-11, 6P-12 and 6P-13, the mean number of grains per unit area, i. e. the grain size was tested. This has enabled subsequent easier and more accurate simulation of the occurrence of crystal grains and their distribution in the cone-shaped measuring cell and in the industrially cast ingot.

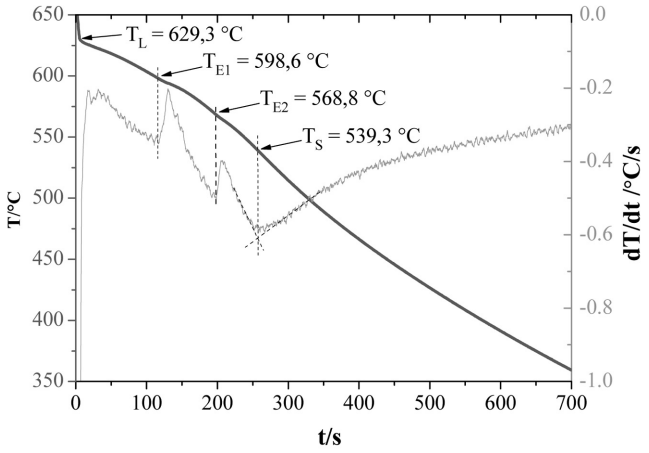

Figure 5. Cooling curve of sample 6P-1-a of EN AW-5083 alloy cast in the measuring cell made by Croning process.

Bild 5. Die Abkühlungskurve der Probe 6P-1-a von der Legierung EN AW-5083, gegossen in die Messzelle, hergestellt durch den Croning Prozess.

Figure 5 shows the cooling curve (blue curve) and its first derivation (red curve) of the tested sample 6P-1a (since two measurements were carried out: a) and b), cast in the measuring cell made by the Croning process. On the cooling curve of the tested sample 6P-1, Figure 5, there are no pronounced peaks due to relatively low cooling rate in the measuring cell made by the Croning process of only 8.3 °C/s. By means of the first derivation of the cooling curve the liquidus and solidus temperatures can be determined, as well as the eutectic temperatures of the tested sample.

From the cooling curve of sample 6P-1 it may be noted that the solidification starts at temperature $T_L = 629.3$ °C. The eutectic solidification of the melt into eutectic *E1* occurs at the temperature of $T_{E1} = 598.6$ °C. At $T_{E2} = 568.8$ °C the second eutectic *E2* occurs. The solidification of sample 6P-1-a ceases at temperature solidus $T_S = 539.3$ °C, so that the obtained time of solidification amounts to $\Delta t_s = 250.1$ s.

3.2 Results obtained by differential scanning calorimetry (DSC)

Differential scanning calorimetry of sample 6P-1 has resulted in heating and cooling curves at velocities of $r_s = 0.17$ °C/s, and its first derivations. *Figure 6* shows the DSC cooling curve for sample 6P-1, DSC. The DSC cooling curve of sample 6P-1, DSC shows that the solidification occurs in the temperature interval between 637.2 °C (T_L) and 527.0 °C (T_S), and due to the lowest cooling rate it needs the longest time for solidification, Δt_s = 660.6 s. The eutectic solidification of the melt into eutectic *E1* occurs at temperature T_{E1} = 595.8 °C, whereas the separation temperature of the second eutectic is $T_{E2} = 569.6$ °C.

3.3 Dependence of solidification time of sample 6P-1 at different cooling rates

Liquidus and solidus temperatures, and the time intervals of solidification of the tested samples in DSC analysis (6P-1, DSC), in the measuring cell made by the Croning process (6P-1, STA), and for individual places in the cone-shaped die cast (6P-13 and 6P-12), following the ascending cooling rate, *Table 2*.

By analysing their dependence the correlation has been obtained between the experimentally determined cooling rates and the achieved solidification times, presented by curve in *Figure 7* and *equation (1)*. The cooling rate shows steep decline to

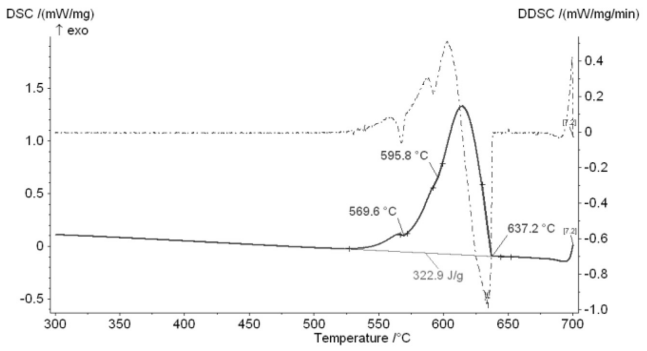

Figure 6. DSC cooling curve of sample 6P-1, DSC alloy EN AW-5083.

Bild 6. DSC-Abkühlkurve der Probe 6P-1, DSC-Legierung EN AW-5083.

Table 2. Significant temperatures of phase changes and times of solidification at different cooling rates of sample 6P-1 of alloy EN AW-5083

Tabelle 2. Signifikante Temperaturen der Phasenänderungen und der Zeiten der Erstarrung mit unterschiedlichen Abkühlgeschwindigkeiten der Probe 6P-1 und der Legierung EN AW-5083

r_c [°C/s]	0.17 (6P-1, DSC)	8.3 (6P-1, STA)	10.8 (6P-13)	40.3 (6P-12)
T_L [°C]	637.2	630.8	632.7	634.0
T_S [°C]	527.0	538.9	540.9	523.7
Δt_s [s]	660.6	250.1	65.0	11.2

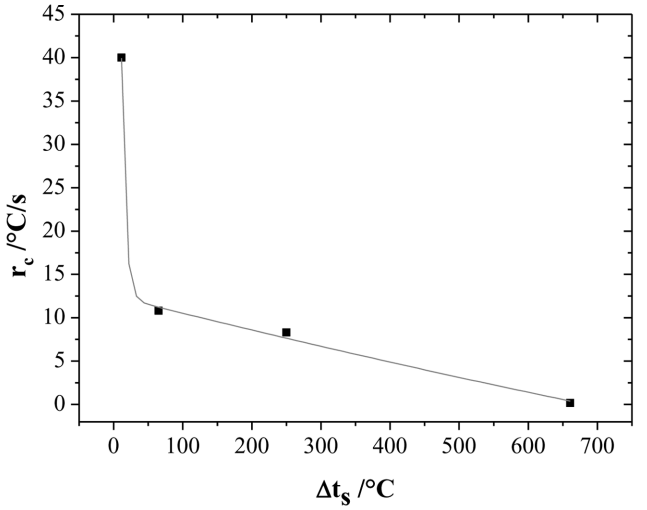

Figure 7. Dependence of cooling rate on time of solidification of sample 6P-1 of alloy EN AW-5083.

Bild 7. Abkühlgeschwindigkeit in Abhängigkeit der Zeit bis zum Erstarren der Probe 6P-1 und der Legierung EN AW-5083.

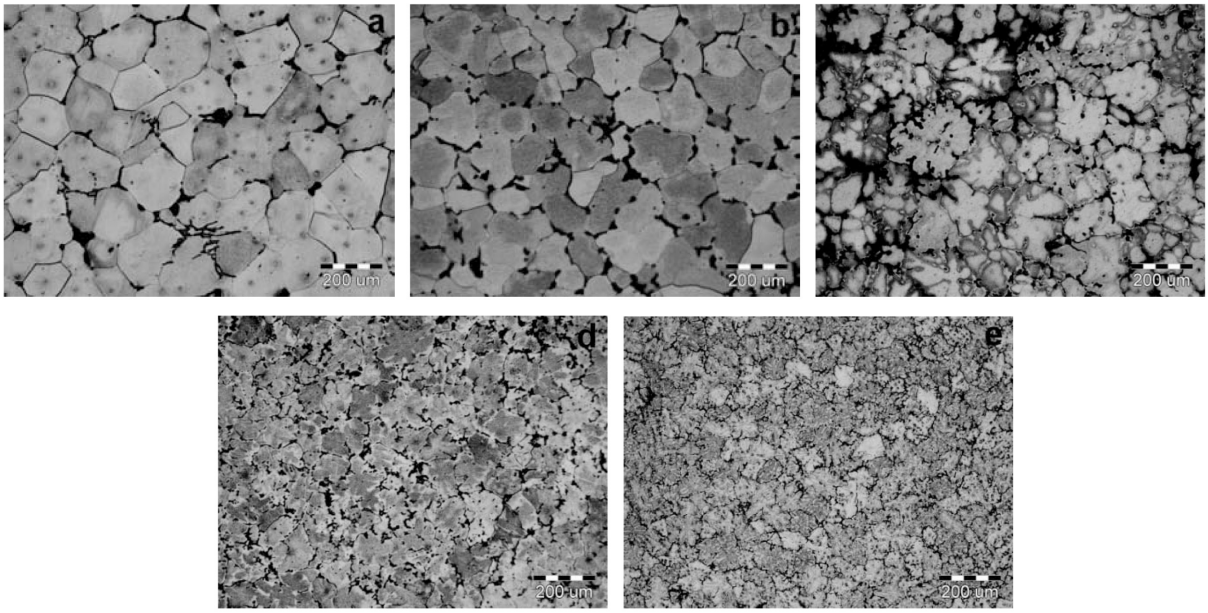

Figure 8. Images of microstructures of EN AW-5083 alloy samples according to increasing cooling rates, etched electrolytically with Barker's reagent, observed with optical microscope (polarized light with sensitive tint filter), magnification 100x, a) Sample 6P-1, DSC at r_c = 0.17 °C/s; b) Sample 6P-1, STA at r_c = 8.3 °C/s; c) Sample 6P-13 cast into cone-shaped measuring cell at r_c = 10.8 °C/s; d) Sample 6P-12 cast into cone-shaped measuring cell at r_c = 40.3 °C/s; e) Sample 6P-11 cast into cone-shaped measuring cell at r_c = 124.0 °C/s.

Bild 8. Mikrostrukturen der Legierungsprobe EN AW-5083 nach steigender Abkühlgeschwindigkeit, elektrolytisch geätzt mit Barker-Reagenz, aufgenommen mit einem optischen Mikroskop (polarisiertes Licht mit empfindlichen Farb-Filter), 100-fach vergrößert, a) Probe 6P-1, DSC bei r_c = 0.17 °C/s, b) Probe 6P-1, JTA bei r_c = 8.3 °C/s, c) Probe 6P-13 aus der kegelförmigen Messzelle bei r_c = 10.8 °C/s, d) Probe 6P-12 aus der kegelförmigen Messzelle bei r_c = 40.3 °C/s, e) Probe 6P-11 aus der kegelförmigen Messzelle bei r_c = 124.0 °C/s.

the time of solidification of 65 s. Above the indicated time of solidification there is lighter, not so steep fall in the cooling rate value. It may be concluded that higher cooling rate leads to pronounced reduction in the time of solidification, i. e. to faster solidification of the alloy, as consequence of greater melt undercooling, i. e. from a thermodynamic aspect, an increase in the driving force of solidification.

Numerical interpretation of the change in the cooling rate on the time interval of solidification is presented by a model given in *equation (1)* with correlation coefficient $R^2 = 0.99$:

$$r_c = 65.96 \cdot \exp(-\Delta t_s/3252.89) + 189.66 \cdot \exp(-\Delta t_s/5.80) - 53.43\ [^\circ C/s] \quad (1)$$

The presented model enables the calculation of the local cooling rates in the industrially semi-continuous cast ingot based on the solidification times obtained by simulating the ingot casting and solidification processes.

3.4 Determining the mean number of grains per unit area, i. e. the grain size at different cooling rates

Microstructural images of samples 6P-1, DSC; 6P-1, STA; 6P-13; 6P-12 and 6P-11 cast at different cooling rates by means of the influence of material and shape of the mould are presented in *Figure 8*. Visual inspection of the microstructure of each individual sample, etched electrolytically by Barker's reagent, and then recorded in the polarized light, shows evenly distributed grains of uniform size with clearly noticeable difference in colour. Comparison of such images in Figure 8 shows an increase in the number of grains with the increasing cooling rate. Thus, the tiniest grains can be noticed in sample 6P-11 that was cooled at the highest rate of r_c = 124.0 °C/s.

Table 3. Mean number of grains per unit area, $\overline{N}_A$ i. e. the ASTM grain size number, *G-number* at different cooling rates

Tabelle 3. Der Mittelwert der Anzahl von Körnern pro Fläche, $\overline{N}_A$ d.h. die ASTM Korngrößenzahl, G-Zahl bei unterschiedlichen Abkühlgeschwindigkeiten

Sample mark	r_c [°C/s]	$\bar{l}$ [µm]	Counts	G-number	$\overline{N}_A$ [No./mm²]
6P-1, DSC	0.17	170.63	530	1.82	27.81
6P-1, STA	8.3	115.10	499	2.95	60.30
6P-13	10.8	107.2	527	3.16	70.42
6P-12	40.3	87.05	526	3.77	107.04
6P-11	124.0	61.65	518	4.76	213.72

For quantification and verification of the visual trend of microstructural constituent grinding with the increase in the cooling rate, the analysis of the mean number of grains per unit area of samples recorded in polarized light was carried out. The ASTM grain size number, *G-number* and the values of the mean number of grains per unit area, $\overline{N}_A$ in dependence on the cooling rate, r_c are presented in *Table 3*. The software calculates automatically the mean linear intercept length, $\bar{l}$ which is used to calculate by

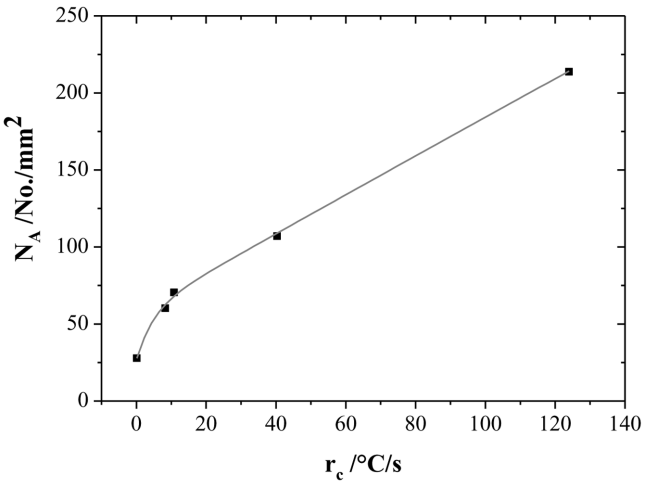

Figure 9. Dependence of the number of grains per unit area on the cooling rate of sample 6P-1.

Bild 9. Abhängigkeit der Anzahl von Körnern pro Fläche auf die Abkühlgeschwindigkeit der Probe 6P-1.

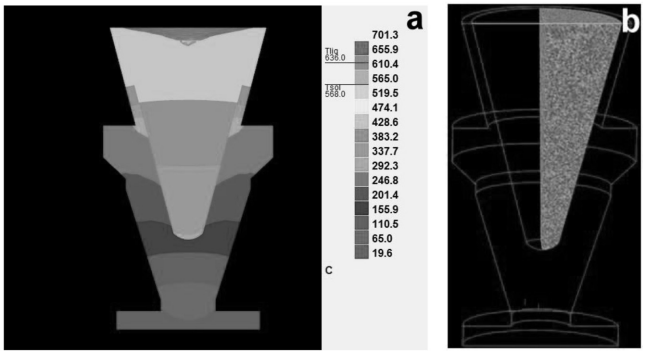

Figure 10. Numerical simulation carried out by "ProCast" simulation software of alloy EN AW-5083 in cone-shaped measuring cell, a) Numerical simulation of temperature field (within time of 80 s since commencement of casting), b) Numerical simulation of occurrence and growth of crystal grains.

Bild 10. Numerische Simulation mit der Simulationssoftware "ProCast" der Legierung EN AW-5083 in der kegelförmigen Messzelle durchgeführt, a) Numerische Simulation des Temperaturfeldes (innerhalb von 80 s seit dem Beginn des Gießens), b) Numerische Simulation der Ereignisse und Wachstum von Kristallkörnern.

means of linear approximation the mean number of grains per unit area tested for the measured *n* areas, $\overline{N}_A$ or *G-number*.

Since the *G-number* changes slightly, the dependence of the mean number of grains per unit area, $\overline{N}_A$ is more pronounced than the cooling rate, r_c. The relation of these parameters is presented in *Figure 9*.

Looking at Figure 9 a sudden increase in the number of grains can be noted with an increase in the cooling rate of up to $r_c \sim 10.8\,^{\circ}C/s$, whereas after this rate the curve features a much smoother slope.

The experimental data for the dependence of the number of grains per unit area, N_A on the cooling rate, r_c can be quantified by the mathematical model of exponential type with correlation factor $R^2 = 1$ (0.99928) as presented by *equation (2)*:

$$N_A = -5161.83 \exp(-r_c/4021.01) - 31.01 \cdot \exp(-r_c/4.80) + 5219.27\ [\text{No./mm}^2] \quad (2)$$

Based on the physical model for N_A, the grain size, *G-number* may be assumed for the tested cooling rate, i. e. type and thickness of the mould wall.

3.5 Numerical simulation of casting, solidification, and development of microstructure for cone-shaped measuring cell

The obtained experimental values of the dependence of the cooling rate and the number of grains were used in the "ProCast" simulation software for the simulation of casting, solidification and development of the microstructure for the cone-shaped measuring cell. The basic parameters required for this simulation are the chemical composition of the EN AW-5083 alloy melt, the starting casting temperature (700 °C), whereas the casting time amounted to 2.2 s.

*Figure 10*a shows the temperature field in the cone-shaped measuring cell in the time period of 80s from the commencement of casting. In the cone-shaped measuring cell the solidification is directed, but nevertheless, uniformly distributed equiaxed grains are obtained, Figure 10b. The performed simulation shows a similar trend of grain distribution and morphology in the cone-shaped sample as well as in the tested actual cast sample of EN AW-5083 alloy.

4 Conclusions

The test results obtained in this paper lead to the following conclusions:

1. Casting of test samples of different shapes and dimensions, as well as types of mould materials made it possible to obtain different cooling rates: by the method of simple thermal analysis by casting into measuring cell made by the Croning process ($r_c = 8.3\,^{\circ}C/s$), whereas casting into cone-shaped measuring cell resulted in achieving three different cooling rates: 10.8 °C/s, 40.3 °C/s and 124.0 °C/s. Differential scanning calorimetry resulted in heating and cooling curves with $r_c = 0.17\,^{\circ}C/s$.
2. Using methods of simple thermal analysis and differential scanning calorimetry the significant temperature phase transitions and times of solidification at certain cooling rates were determined, and the model of dependence of the solidification time on the cooling rate was obtained.

$$r_c = 65.96 \cdot \exp(-\Delta t_s/3252.89) + 189.66 \cdot \exp(-\Delta t_s/5.80) - 53.43\ [^{\circ}C/s]$$

3. It may be concluded that higher cooling rate results in pronounced shortening of the solidification time, i. e. faster solidification of the alloy, as consequence of greater undercooling of the melt, i. e. thermodynamically speaking, increase in the driving force of solidification.

4. Experimental data of the dependence of the number of grains per unit area, N_A on the cooling rate, r_c are quantified by means of a mathematical model of exponential type with correlation factor $R^2 = 1$ (0.99928) as follows:

$$N_A = -5161.83 \cdot \exp(-r_c/4021.01) - 31.01 \cdot \exp(-r_c/4.80) + 5219.27\ [\text{No.}/\text{mm}^2]$$

5. The performed simulation using "ProCast" software package shows a similar trend of grain distribution and morphology in a cone-shaped sample as in the tested real cast sample of EN AW-5083 alloy.

5 References

[1] ASM Specialty Handbook®, Aluminum and Aluminum Alloys, ASM International, Materials Park, Ohio, **2002**.

[2] D. G. Eskin, *Physical Metallurgy of Direct Chill Casting of Aluminium Alloys*, CRC Press/Taylor and Francis Group, Boca Raton, **2008**.

[3] H. E. Vatne, *Aluminium* **1999**, *75*, 84.

[4] H. E. Vatne, *Aluminium* **1999**, *75*, 200.

[5] M. Easton, D. St John, *Solidification of Aluminium Alloys*, The Minerals, Metals and Materials Society, Warrendale, **2004**.

[6] P. D. Lee, R. C. Atwood, R. J. Dashwood, H. Nagaumi, *Mater. Sci. Eng. A* **2002**, *328*, 213.

[7] R. Nadella, D. G. Eskin, Q. Du, L. Katgerman, *Materials Science* **2008**, *53*, 421.

[8] D. G. Altenpohl, Aluminum: Technology, Applications, and Environment, A Profile of a Modern Metal, Aluminum from Within – the Sixth Edition, The Aluminum Association and The Minerals, Metals and Materials Society, Warrendale, **1999**.

[9] *Elements of Metallurgy and Engineering Alloys*, ASM International, Materials Park, Ohio, **2008**.

[10] N. Dolić, *Ph.D. Thesis*, University of Zagreb Faculty of Metallurgy, Sisak, Republic of Croatia, **2010**.

Received in final form: January 26th 2012 T 929

